JOURNAL OF MAGNETIC RESONANCE 43, 399–416 (1981)

A Multinuclear Double-Tuned Probe for Applications with Solids or Liquids Utilizing Lumped Tuning Elements

F. DAVID DOTY, RUTH R. INNERS, AND PAUL D. ELLIS*

Department of Chemistry, University of South Carolina, Columbia, South Carolina 29208

Received August 27, 1980; revised December 1, 1980

A high-efficiency multinuclear double-tuned probe using lumped-element construction is compared and contrasted with a transmission line probe. A rationale for improved efficiency at the high frequency and a commensurate improvement in the signal-to-noise ratio is developed. Powder spectra obtained at 44.4 MHz with the lumped-element probe are shown and pertinent construction details are given.

During the past several years there has been a resurgence of research interest in the liquid-state NMR of nuclides other than ^{1}H, ^{19}F, and ^{13}C. Paralleling this interest in multinuclear high-resolution liquid-state NMR has been the development of high-power pulse equipment and fixed-frequency double-tuned probes capable of performing experiments in solid-state cross-polarization and magic angle spinning in a "routine" manner. Since an essential factor in the rapidly increasing interest in the liquid-state NMR of the less common nuclides can be attributed in part to the commercial availability of high-sensitivity tunable broadband probes a natural question arises: "Can one develop just such a multinuclear probe for solids that is able to withstand sufficiently high power ^{1}H decoupling and at the same time is highly sensitive to the observe nuclide and is capable of magic angle spinning at rates in excess of 3.0 kHz?" The answer is a "qualified" yes. However, before one can explain what is meant by "qualified," it is important to address elements in the design of an NMR probe for solids and to show how these features affect the power requirements and the sensitivity of the probe. The design of a high-speed spinner will be the subject of a separate paper.

The purpose of the present paper is to detail our approach to the development of a high-sensitivity broadband tunable probe used in our laboratory for "high-resolution" experiments on solids. The probe to be described assumes the geometry associated with a 4.7-T wide-bore superconducting magnet, but only slight modifications are necessary to implement our approach on a narrow-bore magnet. The theory is further extended to higher and lower magnetic fields.

Recent approaches to double-tuned NMR probes have tended to favor transmission line tuning (*1*) as opposed to lumped-element tuning because of the difficulty in obtaining high-voltage and high-current capacitors that will fit in the probe for the lumped circuits. This approach imposes severe restrictions on the sample coil

* Author to whom correspondence should be sent.

0022-2364/81/060399-18$02.00/0

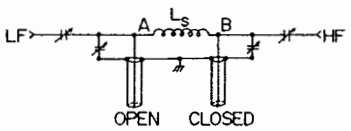

FIG. 1. Double-tuned probe circuit using transmission lines (*1*).

inductance and makes broadband tunable probes very inefficient. We first review some of the details of a typical double-tuned probe using transmission line elements. Then we present a similar circuit using lumped elements and compare the two approaches with regard to efficiency, signal-to-noise ratio, decoupler rejection, power handling, versatility, tunability, and ease of construction. We include data obtained in our laboratory at 44.4 MHz. The next section presents some possibilities for both fixed and variable capacitors and inductors and reviews some useful relationships and design considerations.

THE TRANSMISSION LINE DOUBLE-TUNED PROBE

The advantages of a single-coil double-tuned probe for solid-state rotating-frame experiments are well documented (*2*) and need not be repeated, but the effects of nonideal components in the circuit deserve further comment. For example, let us consider the circuit of Fig. 1, which is commonly used when it is desirable to optimize the signal-to-noise ratio at lower frequency albeit at the expense of high-frequency performance. This network is easy to analyze and allows maximum flexibility in tuning and matching, but requires four extremely high voltage, high current capacitors. In practice, it may be impossible to construct such a probe with the limitations imposed by the bore size of the magnet. Further, if the capacitors are placed outside the magnet, the effects of lead losses would be substantial.

The $\lambda/4$ lines depicted in Fig. 1 are cut to the resonant frequency of the nucleus to be decoupled. Usually this frequency, HF, is higher than the observe frequency, LF, so we limit our discussion to this case. For lossless transmission lines, the closed $\lambda/4$ line at point B presents an infinite impedance at the frequency HF; thus all of the HF rf power is available to the sample coil, L_S. The open $\lambda/4$ line at point A presents zero impedance to the HF and thus serves as a virtual ground for the HF power. As a result there should be no HF power on the LF side of the probe. However, when losses are introduced into the $\lambda/4$ lines, the picture is altered. At point A the impedance is usually large enough (perhaps because of ground loops resulting from several different ground planes) to limit the HF rejection to less than 20 db on the LF side of the probe. But of even greater consequence is the finite impedance presented by the closed $\lambda/4$ at point B in that there is a dramatic loss in HF efficiency. To understand how these losses come about, we employ a series–parallel reduction scheme on an equivalent circuit using lumped elements in place of the $\lambda/4$ lines.

HF Efficiency

Clearly, the objective is to dissipate as much energy in the sample coil as possible. In the subsequent analysis it is important to recall that the losses in a tuned

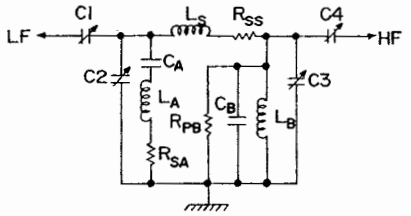

FIG. 2. Lumped-element equivalent of Fig. 1.

circuit can be represented either by a series resistance

$$R_s = X_L/Q = \omega L/Q \quad [1]$$

or by a parallel resistance

$$R_p = X_L Q, \quad [2]$$

where X_L is the inductive reactance.

With this in mind, consider the circuit depicted in Fig. 2, in which the λ/4 lines of Fig. 1 have been replaced by their lumped-element equivalents. Then make the further simplification that the λ/4 lines are precisely at resonance—zero series and infinite parallel impedance—and consider only the HF side. We further assume $X_{C2} \gg R_{SA}$ so that we can neglect the effect of the LF matching components. This should be reasonable except when observing very low γ nuclei.

The series resistance in the sample coil is given by

$$R_{SS} = X_{LS}/Q_S = \omega L_S/Q_S. \quad [3]$$

The series resistance in the open λ/4 is given by

$$R_{SA} = Z_0/Q_A, \quad [4]$$

and the parallel resistance of the closed λ/4 is given by

$$R_{PB} = Z_0 Q_B. \quad [5]$$

We can now make the HF approximation shown in Fig. 3, where the sample coil and the open λ/4 line are combined to give a total series inductance

$$L_{SA} = L_S + L_A \quad [6]$$

with an effective parallel resistance of

$$R_{PSA} = (X_{LS} + X_{LA})Q = \frac{(X_{LS} + X_{LA})^2}{R_{SS} + R_{SA}}, \quad [7]$$

where $X_{LA} = X_{LB} = Z_0$.

To obtain high efficiencies in delivering rf power to the sample coil, the resistance of the closed λ/4, R_{PB}, must be large compared to the combined impedance presented by the sample coil and the open λ/4, R_{PSA}, since the former is in parallel with the latter. Furthermore, to assure that most of the power is dissipated in the sample coil, the series resistance of the sample coil, R_{SS}, must be large compared to the series resistance of the open λ/4, R_{SA}, since the former is in series with the latter. It is easy to show that the overall HF efficiency, η_{HF}, defined as the

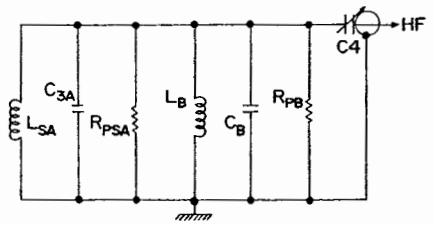

FIG. 3. HF approximation of Fig. 2 at resonance.

fraction of power dissipated in the sample coil alone, is given by

$$\eta_{HF} = \frac{R_{SS}}{(R_{SS} + R_{SA})} \frac{R_{PB}}{(R_{PB} + R_{PSA})} \quad [8]$$

or

$$\eta_{HF} = \frac{X_{LS} Z_0 Q_A}{(X_{LS} Q_A + Z_0 Q_S) Z_0 + (Z_0 + X_{LS})^2 Q_S} \quad [9]$$

when $Q_A = Q_B$.

The above equation does not readily simplify except in certain limiting conditions; so to give the reader a more concrete feeling for the effect of the various resistances, the following typical case is presented: HF = 200 MHz, $Z_0 = 50\ \Omega$; $L_S = 200$ nH; $Q_S = 250$; $X_{LS} = \omega L_S = 250\ \Omega$;

$$Q_A = Q_B \simeq 18\nu^{1/2}\ (\text{MHz})^{-1/2} = 250. \quad [10]$$

The frequency dependence of the Q of the $\lambda/4$ lines arises from the frequency dependence of the surface resistance of a conductor (Table 1). The coefficient is determined empirically for an 8-mm low-loss semirigid line.

Since all the Q values are assumed equal, Eq. [9] simplifies to

$$\eta_{HF} = \frac{X_{LS} Z_0}{(X_{LS} + Z_0) Z_0 + (Z_0 + X_{LS})^2} \simeq 12\%. \quad [11]$$

It can be shown that for $Q_A = Q_B = Q_S$ the maximum achievable HF efficiency is 17% and it is obtained when X_{LS} is chosen equal to $1.4Z_0$. Higher "efficiencies" are possible if the Q of the sample coil is reduced but this actually results in a reduction of the rf field strength. Real increases in the efficiency of the production of rf fields are attainable only when the Q values are increased by using larger $\lambda/4$ lines or when the open $\lambda/4$ line is eliminated. By substituting high-Q lumped elements, it is possible to get efficiencies of 50% or better on the HF side; but before examining this possibility, we turn to the problem of broadband tuning of the LF side of the transmission line probe.

Broadband Tuning of the Observe Frequency

By saying "broadband" we do not mean to imply a low-Q probe, but rather that the frequency can be tuned over a wide range—for example, one-half octave—while maintaining a good match. This requires the total capacitance on the observe side—C_1 plus C_2 plus C_A plus stray capacitance—to change by a factor of 2. If we

TABLE 1

THE SURFACE RESISTANCE AND SKIN DEPTH[a] FOR SEVERAL CONDUCTORS AS A FUNCTION OF THE SQUARE ROOT OF THE FREQUENCY

Material	ρ_s ($\mu\Omega.Hz^{-1/2}$)	δ (cm $Hz^{1/2}$)
Silver[b]	0.25	6.4
Copper	0.26	6.5
Gold	0.31	7.7
Aluminum	0.32	8.2
Brass	0.51	13
Tin–lead solder	0.78	20
Stainless steel	2.0	49

[a] The surface resistance and skin depth can be calculated from $\rho_s = (\sigma\delta)^{-1}$ and $\delta = (2/\omega\mu\sigma)^{1/2}$, where σ is the electrical conductivity (*3*).

[b] The values given for silver apply only to annealed fine silver. Cyanide-plated silver is generally inferior to copper at UHF.

select a 3 to 30-pf capacitor for C_2 since apparently that is the only choice available in small 15-kV vacuum variables, then the total capacitance must have a maximum value of 54 pf to allow a factor of 2 change in capacitance. The stray capacitance will typically be 1 to 2 pf for the coil plus 2 to 4 pf for a vacuum variable. The capacitance of the open $\lambda/4$ line at resonance is given by

$$C_A = 1/\omega_0 Z_0. \quad [12]$$

But the capacitance and inductance of a resonant transmission line are reduced compared to values below resonance. Clearly this is to be expected because of the voltage and current distribution. In fact, the capacitance and inductance increase by about 50% at frequencies well below resonance; thus

$$C_A \simeq 1.5/\omega_0 Z_0 \simeq 24 \text{ pf} \quad [13]$$

for a 200-MHz, $\lambda/4$, 50-Ω line below resonance.

It can be shown that the matching capacitor C_1 is required to have an impedance equal in magnitude to the geometric mean of the resistances to be matched (analogous to antireflective coatings on lenses). Since this capacitance is small compared to the total capacitance when $R_p \gg Z_0$ (as is always the case at high frequencies) it is easily shown that

$$C_1 \simeq (C_2/Q\omega Z_0)^{1/2} \simeq 4 \text{ pf}. \quad [14]$$

Thus the total maximum capacitance is about 60 pf and the tuning range is a little less than one-half octave. To extend the tuning range of the probe one must find a small high-current variable capacitor with more capacitance, or decrease C_A by using a higher-impedance open $\lambda/4$ line, or remove the open $\lambda/4$ and use some other means to get the desired HF rejection.

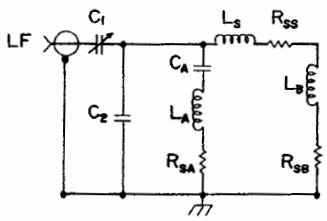

FIG. 4. LF approximation of Fig. 2.

We examine the latter possibility shortly, but first let us consider the effect of the $\lambda/4$ lines on the LF from the approximation shown in Fig. 4. Note that we have dropped C_B. We ignore its small effect except to say that when properly included, it makes L_B and R_{SB} appear larger by $(1 + (LF/HF)^2)$ and the efficiency is slightly reduced. The inductance of the closed $\lambda/4$ line at resonance is given by

$$L_B = Z_0/\omega_0. \qquad [15]$$

Again at frequencies well below resonance, the inductance increases by about 50%. Thus, for example, a 200-MHz, closed $\lambda/4$, 50-Ω line below resonance has an inductance of about 60 nH. The inductance at low frequency of the open $\lambda/4$ is about half that of the closed $\lambda/4$, or about 30 nH. The total inductance is determined so as to resonate with the maximum capacitance at the minimum observe frequency. For example, a 260-nH total inductance will tune from about 40 to about 55 MHz with a 30-pf variable capacitor. Thus we choose a sample coil with an inductance of about 200 nH to give a total inductance of 260 nH since it is in series with L_B. Earlier we showed that this much inductance in the sample coil resulted in an efficiency of only 12% for the HF at 200 MHz. Reducing the inductance of the sample coil to 60 nH would raise the HF efficiency to about 17%, assuming the Q is not degraded; but now an additional 60-pf capacitor is required in parallel with C_2, the tuning range is reduced to a 17% frequency change, and the LF efficiency is reduced to 40%, as is shown in the next section.

LF Efficiency

Fortunately, the losses at the observe frequency are much less devastating since the full resonance current now flows through the sample coil. At the maximum observe frequency we can neglect the small current flowing in C_1 and C_2 and the efficiency is seen from Fig. 4 to be

$$\eta_{LF} = \frac{R_{SS}}{R_{SS} + R_{SB} + R_{SA}}. \qquad [16]$$

At the minimum observe frequency, about half the current flows through C_2 and about half flows through C_A. The efficiency is then

$$\eta_{LF} = \frac{R_{SS}}{R_{SS} + R_{SB} + R_{SA}/4}. \qquad [17]$$

Since the surface resistance of a conductor is proportional to the square root

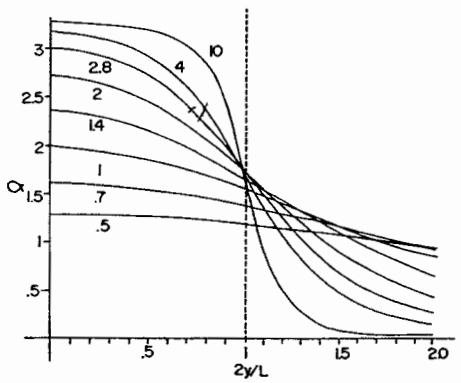

FIG. 5. Axial component of rf magnetic field on axis for several ratios of length to radius in solenoids as a function of normalized distance from the center.

of the frequency, the low-frequency series resistances are proportional to the product of the square root of the ratio of the frequencies and the high-frequency series resistances.

If we use conditions identical to those of the previous example, the efficiency is about 70% at the maximum frequency and 75% at the minimum frequency. But if we lower the sample coil inductance to 60 nH so as to improve the HF efficiency, the LF efficiency drops to 40%. These losses arise primarily from the closed $\lambda/4$. They are greater at the higher frequency because the open $\lambda/4$ is not a high-Q capacitor.

Relationship between Efficiency and S/N

Let us consider the effect of the sample coil in series with a second empty coil. It can be shown from the principle of reciprocity (*4*) that for a given sample and given temperature, the signal voltage generated in the sample coil is

$$\xi_s \propto B_1 V_s \nu^2 / I, \qquad [18]$$

where B_1 is the transverse rf field strength generated in the sample coil with current I and sample volume V_s. The total thermal noise from the two coils with effective series resistance R is

$$\xi_n \propto (\Delta\nu R)^{1/2}, \qquad [19]$$

where $\Delta\nu$ is the overall bandwidth. Thus for a given bandwidth, temperature, and sample,

$$\frac{S}{N} \propto \frac{B_1 V_s \nu^2}{I R^{1/2}} = \frac{B_1 V_s \nu^2}{P^{1/2}}, \qquad [20]$$

where P is the total power.

Now recall that the Q is the ratio of energy stored to energy dissipated per radian; hence for the sample coil with inductance L_S and power efficiency η

$$Q_S = \frac{(1/2) I^2 L_S \omega}{\eta P}. \qquad [21]$$

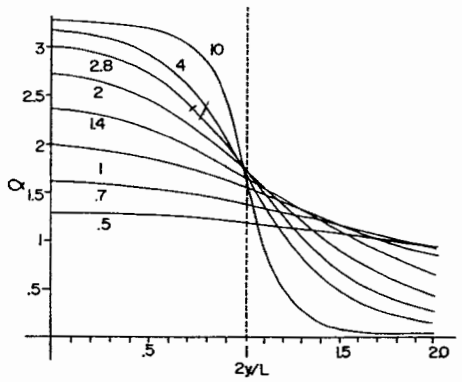

FIG. 5. Axial component of rf magnetic field on axis for several ratios of length to radius in solenoids as a function of normalized distance from the center.

of the frequency, the low-frequency series resistances are proportional to the product of the square root of the ratio of the frequencies and the high-frequency series resistances.

If we use conditions identical to those of the previous example, the efficiency is about 70% at the maximum frequency and 75% at the minimum frequency. But if we lower the sample coil inductance to 60 nH so as to improve the HF efficiency, the LF efficiency drops to 40%. These losses arise primarily from the closed $\lambda/4$. They are greater at the higher frequency because the open $\lambda/4$ is not a high-Q capacitor.

Relationship between Efficiency and S/N

Let us consider the effect of the sample coil in series with a second empty coil. It can be shown from the principle of reciprocity (*4*) that for a given sample and given temperature, the signal voltage generated in the sample coil is

$$\xi_s \propto B_1 V_s \nu^2 / I, \qquad [18]$$

where B_1 is the transverse rf field strength generated in the sample coil with current I and sample volume V_s. The total thermal noise from the two coils with effective series resistance R is

$$\xi_n \propto (\Delta\nu R)^{1/2}, \qquad [19]$$

where $\Delta\nu$ is the overall bandwidth. Thus for a given bandwidth, temperature, and sample,

$$\frac{S}{N} \propto \frac{B_1 V_s \nu^2}{I R^{1/2}} = \frac{B_1 V_s \nu^2}{P^{1/2}}, \qquad [20]$$

where P is the total power.

Now recall that the Q is the ratio of energy stored to energy dissipated per radian; hence for the sample coil with inductance L_S and power efficiency η

$$Q_S = \frac{(1/2) I^2 L_S \omega}{\eta P}. \qquad [21]$$

But,

$$(1/2)I^2L \propto B_1^2 V_c, \quad [22]$$

where V_c is the volume of the coil, and the constant of proportionality depends on the coil geometry. From Eqs. [21] and [22] we see that

$$B_1 = \alpha(\eta Q_s P/\nu V_c)^{1/2}. \quad [23]$$

A more complete analysis allows an exact determination of α for certain coil geometries. Figure 5 shows α as a function of distance from the center of the coil for solenoids of several different ratios of length to radius. The field strength in Eq. [23] is in gauss when the volume enclosed by the coil is in cubic centimeters, ν is in megahertz, and P is in watts.

Substituting Eq. [23] into Eq. [20] yields

$$\frac{S}{N} \propto \left(\frac{\eta Q_s}{V_c}\right)^{1/2} V_s \nu^{3/2}. \quad [24]$$

The above equation is valid for a given sample material, coil geometry, and temperature, and it is sufficient for the present purpose of showing the effect of the efficiency on the signal-to-noise ratio. For example, an efficiency of 70% results in a 16% reduction of S/N, or requires a 35% increase in spectrometer time for the same S/N ratio.

THE LUMPED-ELEMENT DOUBLE-TUNED PROBE

Now we consider a similar circuit in which the transmission lines have been replaced by lumped elements, but the values of the components are no longer constrained to the equivalent values of 50-Ω, λ/4 lines. From Eq. [8] it is clear that the HF efficiency can be improved by increasing R_{PB}/R_{PSA} and by increasing R_{SS}/R_{SA}. Clearly, R_{SA} should be reduced to as near zero as possible. Alternatively, we can eliminate the λ/4 line and still assume point A to be a virtual ground at the HF since the parallel reactance of C_3 plus C_4 is much less than the reactance of the sample coil at the HF. The effect of the nonzero reactance at point A is to slightly reduce the effective inductance of the sample coil at the HF. The small reactance of C_3 plus C_4 is subtracted from the larger inductive reactance of L_S. We assume the series resistances of C_3 and C_4 to be negligibly small.

Heretofore, we have frequently simplified the relationships by assuming the Q values of the various inductors to be equal. However, since L_B is not constrained to the same limiting geometry as the sample coil, a more realistic simplification with lumped elements may be to assume Q_B to be 50% more than Q_S. Now with the open λ/4 gone as shown in Fig. 6, the following expressions follow directly from Eqs. [8] and [16],

$$\eta_{HF} \simeq qL_B/(L_S + qL_B), \quad [25]$$

$$\eta_{LF} \simeq qL_s/(qL_s + L_B), \quad [26]$$

where

$$q = Q_B/Q_S \simeq 1.5. \quad [27]$$

Thus, if we make L_S equal to L_B, we obtain efficiencies of about 60% at both fre-

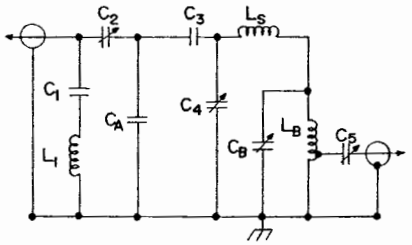

FIG. 6. Double-tuned probe circuit using lumped elements.

quencies; but we may desire to increase L_S to twice L_B for improvement in efficiency to 75% at the observe frequency at the expense of reducing the decoupling efficiency to 43%. For large sample volumes with solenoid coils, the sample coil quality, Q_S, may be nearly equal to the stop coil quality Q_B. Replacing the q values in Eqs. [25] and [26] with a lower ratio of Q_B to Q_S will decrease both efficiencies and may make it desirable to increase further the ratio of L_S to L_B to maintain a high LF efficiency and near-optimum sensitivity.

The Sample Coil Inductance

Having eliminated the $\lambda/4$ lines we now have more freedom in our choice of the sample coil inductance. There are several reasons for choosing inductances higher than those commonly reported. First, the number of turns must be greater than the ratio of the length to the radius of the sample coil, or homogeneous rf fields over most of the coil volume are difficult to achieve and the Q is degraded. The inductance of a solenoid of length l and radius r (cm) with n turns is given by

$$L \simeq 40n^2 \frac{r^2}{l + 0.9r} \text{ nH/cm.} \qquad [28]$$

Thus, except for certain novel coil designs being developed in our laboratory, the above restriction places a minimum value on the inductance of

$$L > 0.05 V_c^{1/3} \ \mu\text{H/cm,} \qquad [29]$$

where V_c is the volume of the coil in cubic centimeters. Thus the advantage of a large sample volume necessitates a larger inductance. Second, a larger inductance means lower lead losses, which often results in higher Q and lower rf leakage fields. And finally, capacitors with small vacuum variables are available only in low-capacitance, high-voltage ranges; thus, high inductances are required for broad-band tuning.

Of course, there are an equal number of disadvantages in going to higher inductances. First, increased dielectric losses in the sample will make the tuning more sample dependent and may lower the Q with certain samples. Second, the Q of the coil will decrease as the capacitance between windings approaches that required for self-resonance. And finally, spatial limitations may make it very difficult to avoid arcing with the increased voltages of high-inductance coils.

It is generally advisable to choose an integral number of turns that requires a

TABLE 2

THE HIGH-FREQUENCY AND LOW-FREQUENCY EFFICIENCIES FOR SEVERAL RATIOS OF THE SAMLE COIL INDUCTANCE TO THE STOP COIL INDUCTANCE[a]

	L_S/L_B			
	1	2	3	4
η_{HF} (%)	60	43	33	27
η_{LF} (%)	60	75	82	86
$(\eta_{LF})^{1/2}$ (%)	77	87	91	93

[a] These values assumed a ratio of Q values to be 1.5 (see Eqs. [25] and [26]).

minimum tuning capacitance much greater than the stray capacitance. We first tried 600 nH to allow nearly a full octave of tuning range with a 30-pf variable on the observe side, 30 to 54 MHz, but excessive problems with arcing above 200 W forced us to change to 200 nH and accept the reduced tuning range.

Matching Networks

There are many possible matching networks that have advantages over the one illustrated in Fig. 1 in that the demands on the matching variable capacitors are reduced and tuning is simplified. Figure 6 shows one such possibility in which a capacitive divider is used on the observe side and an inductive divider is used on the decoupling side. The open $\lambda/4$ line has been replaced by C_A where $C_A > C_3$. The closed $\lambda/4$ line has been replaced by L_B (two turns, tapped one-third turn from ground) and C_B. In both cases, the matching voltage is reduced by a significant factor. Thus the matching capacitance must be increased but at a proportionally lower voltage. However, the size and cost of capacitors generally scale as CV^2; thus the cost and volume of the matching variables are reduced. Two other significant benefits are the reduced frequency dependence (*5*) of the matching variables and the reduced interaction of the matching adjustments with the frequency adjustments.

The additional capacitor at the LF input, C_1, is selected to have a reactance of about Z_0 at the decoupling frequency. It is tuned with L_1 to keep the HF from entering the observe line. In order for it to be effective, it must be positioned very close to the end of the LF line. It also acts as a partial bypass at the higher observe frequencies. This results in less frequency dependence in the matching capacitor, C_2, but its capacitance must now be increased slightly. The losses introduced by C_1 and L_1 are negligible at both the LF and HF since only a small fraction of the resonant current flows through this trap.

The LF tuning range of the probe can now be extended since C_3 plus stray capacitance can easily be made half as large as the capacitance of the open $\lambda/4$ line in Fig. 2, and this allows the frequency adjustment to have a more significant

effect. The minimum value of C_3 is determined by the criterion that C_A be larger than C_2 to keep the frequency dependence of C_2 down and to reduce its voltage requirements. Of course, the sample coil and stop coil inductances must be increased appropriately.

Comparing the Two Approaches

We stated earlier that the maximum HF efficiency for a transmission line double-tuned probe is about 17%. The LF efficiency obtained with this sample coil inductance is less than 40% and the tuning range is only 17%. By increasing the sample coil inductance, we were able to increase the observe efficiency to 75% and the tuning range to 40%. However, the decoupling efficiency dropped from 17 to 12%. On the other hand, when high-Q lumped elements are used, one can control the efficiencies at the two frequencies by the choice of L_S and L_B, as summarized in Table 2. The result is a high-performance broadband probe.

The implications on power requirements are obvious since the power required for a given 90° pulse with a given sample coil geometry is inversely proportional to the efficiency and Q. Furthermore, the implications on signal to noise are equally obvious since we have shown that the S/N is proportional to the square root of the efficiency. Thus, the lumped-element probe shown in Fig. 6 with $L_S = 2L_B$ has an observe S/N a few percent better than the transmission line probe of Fig. 1 and requires less than one-third the decoupling power. Furthermore, it tunes over a broader range and has much better HF rejection on the observe side. Admittedly, the advantages of the lumped-element approach become less significant at higher frequencies because the Q of the $\lambda/4$ line increases. Likewise there is less advantage in our approach with smaller sample coils because the Q of a small sample coil could be much less than the Q of the $\lambda/4$ line.

An $L_S = 2L_B$ powder probe is operating in our laboratory at 50.32 MHz ^{13}C, 44.4 MHz ^{113}Cd and double tuned for ^1H at 200 MHz. The measured 90° pulse widths at the indicated power levels are shown in Table 3. The 5.5-μsec 90° pulse for ^{13}C represents a 42-G B_1 field. To achieve the Hartman–Hahn match condition necessary for cross-polarization via spin lock, a 10-G B_2 field is needed. The power requirements for this experiment are about 150 W for ^{13}C and less than 40 W for ^1H.

TABLE 3

MEASURED 90° PULSE WIDTHS AT INDICATED POWER LEVELS FOR A 2:1 PROBE

Power (W)	Pulse width (μsec)
^1H	
90	3.4
40	5.2
^{13}C	
156	5.5

FIG. 7. ^{113}Cd spectrum of CdS_2; one-scan 90° flip angle, 80-msec acquisition time (a) without ^1H irradiation, (b) with ^1H irradiation.

The loaded Q measured at 50.32 and 44.4 MHz is 250 and at 200 MHz is 400. The 90° pulse widths are approximately equal for both nuclides. The sample coil volume is about 1.7 cm^3 with a length-to-radius ratio of about 2.5. From Eq. [24] and Fig. 5 we expected observe field strengths of about 50 G near the center of the coil and 31 G near the ends of the coil for the above conditions at the observe frequency. This agrees very well with the experimentally determined average value of 42 G.

No discernible loss in signal to noise is observed as shown in the spectra of CdS_2 obtained without (Fig. 7a) and with (Fig. 7b) about 100 W ^1H decoupling power. This fact is attributed to the 35-db HF rejection in the probe plus additional external low-pass filters.

We obtain routine spectra on simple systems such as cadmium salts in which the rate-limiting step is operator efficiency at changing samples, but to assure overnight utilization of the spectrometer, stable long-term acquisition is desirable. The spectrum of cadmium acetate (Fig. 8) represents a 7.5-hr total acquisition time. Longer continuous acquisitions have been obtained with no breakdown in the components in the probe.

RADIOFREQUENCY COMPONENT DESIGN

Before attempting to design a probe, one should be reasonably familiar with the relevant electromagnetic theory and with the practical techniques common to amateur radio. The first four chapters plus Chapter 9 of Poole's experimental treatise "Electron Spin Resonance" (*6*) survey the necessary theoretical background at a level appropriate for an advanced physics undergraduate. The first seven chapters of "The Radio Amateur's Handbook" (*7*) contain many useful equations and practical guidelines. The present section of this paper contains some additional important considerations that are frequently overlooked in the construction of coils and capacitors.

Self-Resonance of Solenoids

In many solids experiments it is important that the spatial dependences of the two rf fields of different frequencies within the sample region be identical to within 0.2% or better. This condition is easily met by a single coil that is double tuned as long as the upper frequency is well below the self-resonant frequency. Except for very high impedance coils, this is seldom a problem. For an unbalanced single-layer

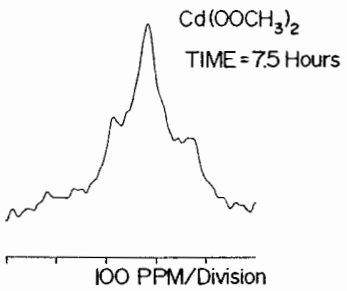

FIG. 8. ^{113}Cd spectrum of $Cd(OOCCH_3)_2$; 15° flip angle, 80-msec acquisition time, 10-sec recycle time.

solenoid with its length approximately equal to its diameter and with the space between adjacent turns approximately half the diameter of the wire, self-resonance occurs when its reactance is around 600 Ω. The self-resonant frequency of a balanced solenoid will be about 50% higher. Generally speaking, the free space wavelength of the self-resonant frequency will be three to five times the conductor length for an unbalanced solenoid, and it will be two to three times the conductor length for a balanced solenoid.

The spatial dependence of the ratio of the rf fields can also be altered by the presence of the stop coil L_B if these coils are not shielded from each other. This requires very high voltage feedthrough capacitors between the separate compartments. They will be discussed later, but first some more remarks about the coils.

High-Q Coils

It is important that Q_S be as high as possible to prevent excessive heating of the sample during the generation of intense rf fields and to increase the sensitivity. The stop coil should also be of high Q for reasons previously mentioned. The coils should be as large as is convenient (but not self-resonant) and made of high-purity copper wire or foil. Heavy silver or gold plating may decrease the Q (*8*), but a thin plate ($\sim 10^{-5}$ cm) is advisable for preventing corrosion. Unnecessary solder plating of conductors should be avoided because of the high resistivity of solder. The following expression is useful for estimating the Q of a solenoid for frequencies well below self-resonance when radiation losses have been eliminated by low-loss shielding that is at least one coil radius away from the coils and the conductor diameter is greater than eight times the skin depth,

$$Q \simeq \frac{0.08\nu^{1/2}rl}{x\rho_s(l + 0.9r)}\ \mu\Omega/\text{cm}. \qquad [30]$$

The surface resistance, ρ_s, and the skin depth, δ, are given in Table 1 for several materials, and x is equal to the distance between centers of adjacent turns divided by the wire diameter. Maximum Q per volume is usually obtained when (*9*)

$$l \simeq 1.4r, \qquad [31]$$

but the requirement that the rf fields be reasonably homogeneous over the sample volume and decrease rapidly outside the sample region is more easily met when the

coil length is increased to several times the coil radius, as seen from Fig. 5. The overall Q of an L-C tank is the reciprocal of the sum of the reciprocal of the Q of the inductor and the reciprocal of the Q of the capacitor. At frequencies below 100 MHz the capacitors generally have higher Q values than the inductors, but at higher frequencies the capacitor Q may seriously limit the total Q unless care is used in the selection and installation of the capacitors.

Power Ratings

A subtle point which deserves understanding is the effect of the thermal cycling produced by the rf pulses. From Eq. [23] it is clear that the ratio of the power levels required at the two frequencies is inversely proportional to the ratio of the Q values. But the Q is inversely proportional to the temperature because of the temperature coefficient of the resistance. The rates of temperature increases of L_S and L_B must then be equal during the pulse, and they must cool down at the same rate following the pulse if the rf field ratio is to remain constant. If the ratio of rf fields in the lumped-element probe described earlier is to remain constant within 0.2%, it can be shown that the temperatures of the coils must track within about 30°C. This sets a lower limit on the mass of the coils unless provision is made to rapidly dissipate the heat generated during the pulse by bonding the coil to a suitable high-thermal-conductivity ceramic such as boron nitride or aluminum oxide. The minimum volume of the conductor required when the heat sink in not provided is

$$V > 0.01Pt \text{ cm}^3/\text{J}, \qquad [32]$$

where P is the power delivered to the coil during the pulse for t sec. For example, a 400-W pulse at 50% efficiency for 50 msec requires a minimum of 0.1 cm^3 of copper, silver, gold, etc., in the coil. (The volume-specific heat of most solids is about 3.5 J/cm^3 K.) This condition requires a minimum thickness of about 0.05 cm for a coil of radius 0.7 cm and length 1.5 cm. That is about 100 times the skin depth at 200 MHz.

The detuning caused by the decrease in Q during the pulse followed by a recovery after the pulse amounts to more than a 5% change in the voltage standing-wave ratio in the above case. This may be intolerable for relaxation experiments and hence will require more massive coils.

It is difficult to make any meaningful comments about the average power-handling capability of a coil because of the strong dependence on air flow. This limit is best determined empirically for each probe, but 0.1 W/°C is probably of the right order of magnitude for a medium-sized NMR coil. Assuming this thermal conductivity, a 200-W, 10-msec pulse at 50% efficiency every second would raise the average temperature 10°C.

Variable Inductors

At high powers and low reactances it may be easier to make a variable inductor than a variable capacitor—at least when only a small frequency adjustment is required. Since this is the case on the high-frequency side of the probe (L_B and C_B), it may be desirable to use a fixed capacitor for C_B and a variable inductor L_B.

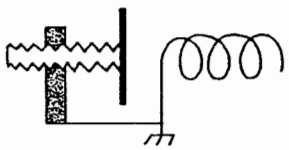

FIG. 9. A variable inductor.

Figure 9 illustrates one possible way of making a nonmagnetic variable inductor. As the conducting disk is moved closer to the coil, the opposing currents induced in it are increased. This reduces the inductance of the coil. If the disk is made of copper or silver, the decrease in Q will be minimal—comparable to the decrease in inductance. The disk should be positioned on the low-potential side of the coil or else well isolated from ground to minimize its capacitive loading since this effect tends to negate the effect of the inductance change.

Capacitor Ratings

Recall that the capacitance of a parallel plate capacitor of surface area A and separation d is given by

$$C = k\epsilon_0 A/d, \qquad [33]$$

where ϵ_0 (0.0885 pf/cm) is the permittivity of free space. The peak voltage that the dielectric can withstand in very thin films ($\sim 10^{-6}$ cm) is generally proportional to the film thickness. However, as the film thickness increases ($\sim 10^{-4}$ cm) the breakdown voltage increases less rapidly—proportional to the square root of the thicknesses—until it approaches the breakdown voltage of air at thicknesses of several centimeters at high frequencies (*10*, *11*). Electric field concentrations near conductor boundaries and flashover may limit the maximum voltage to even lower values. For comparison purposes it is convenient to tabulate typical dc breakdown strengths, E_B, of dielectrics at thicknesses of about 0.5 mm. The peak voltage in an L-C tank of total quality Q at power P is given by

$$V = (2PR_p)^{1/2}. \qquad [34]$$

The peak energy a capacitor can store is given by

$$E_c = CV^2/2. \qquad [35]$$

At resonance $I^2L/2 = CV^2/2$; thus from Eq. [21] the peak power an ideal capacitor can handle is

$$P = E_c\omega/Q. \qquad [36]$$

However, losses may limit the power to a much lower value. The dielectric loss in a capacitor employed in an L-C resonant circuit with overall quality Q, power P, and loss tan δ is given by

$$P_d = PQ \tan \delta. \qquad [37]$$

The I^2R conductor losses in a well-constructed high-power capacitor should be less than the dielectric losses, though this is not the case in small capacitors—especially when the reactance is less than 100 Ω. The dielectric losses and conduc-

TABLE 4

REPRESENTATIVE VALUES OF DIELECTRIC CONSTANT, BREAKDOWN VOLTAGE AT 0.5 mm, AND tan δ FOR SEVERAL HIGH-Q DIELECTRICS

Material	K	E_B (kV/mm)	(tan δ) $\times 10^4$
Vacuum[a]	1	∞	0
Air[a]	1.0006	3	0.001
Quartz[b]	3.8	10	1
BN[c]	4.4	12[c]	5
Porcelain (zicron)[b]	8	12	5
Teflon[a]	2.1	30	2
Polyethylene[a]	2.3	40	2
Polypropylene[a]	2.25	40	5
Mica[b]	6	100	10
Sapphire[c]	9	160	1

[a] Data taken from Ref. (*12*).
[b] Reference (*3*).
[c] Data obtained from Union Carbide Corporation.

tor losses can be combined into a capacitor quality Q_c given by

$$Q_c = (R_s \omega C)^{-1}. \quad [38]$$

At low frequencies the Q of a capacitor is simply $(\tan \delta)^{-1} \sim 2000$, but at high frequencies the conductor losses become significant and the Q drops rapidly. Typical Q values of small chip capacitors at 200 MHz are about 200 for 10-pf chips, and the Q decreases linearly with increasing frequency and capacitance. However, high-power transmitting-type capacitors may have Q values as high as 2000 at UHF frequencies. Table 4 gives representative values of k, E_B, and tan δ several high-Q dielectrics.

The energy that can be absorbed by a capacitor during a pulse is limited by the thermal mass and the maximum operating temperature of the capacitor. This is seldom a serious limitation, but the average power dissipation rating of the capacitor may be a concern. The power dissipated by a capacitor of quality Q_c in a circuit of overall quality Q is

$$P_c = QP/(Q + Q_c), \quad [39]$$

where P is the average input power.

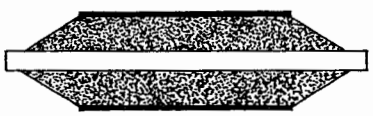

FIG. 10. A coaxial feedthrough capacitor made from two short lengths of copper tubing and an annular piece of low-loss dielectric.

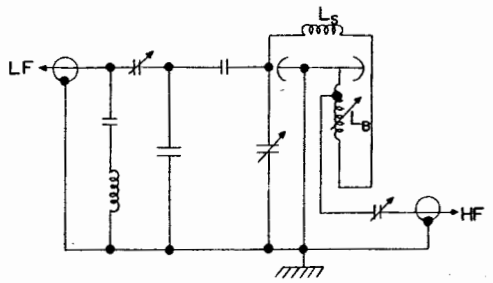

FIG. 11. Final probe circuit using lumped elements, feedthrough capacitors, and a variable inductor.

Feedthrough Capacitors

As mentioned earlier, feedthrough capacitors are required to provide maximum isolation between the sample coil and the stop coil in the interest of achieving identical spatial dependences of the LF and HF rf fields in the sample region. Since we are unaware of a supplier of feedthrough capacitors of appropriate voltage and current ratings, we review some fundamental relationships to assist the interested reader in the construction of his own.

The capacitance of a coaxial line is given by

$$C \simeq \frac{2\pi k \epsilon_0 (l + 2r_0)}{\ln (r_0/r_i)} \qquad [40]$$

and the inductance is given by

$$L \simeq \frac{\mu_0 \ln (r_0/r_i) l}{2\pi}, \qquad [41]$$

where r_0 and r_i are the radii of the dielectric and the inner conductor, respectively. The feedthrough is usually short enough to neglect the inductance and the series resistance. The dielectric thickness $(r_0 - r_i)$ must be great enough to prevent electrical breakdown, which will tend to occur first at the ends. The voltage rating can be improved by carefully insulating the ends of the shield with Teflon film tape to reduce the tendency to arc in this region of concentrated field. The field concentration can be further reduced by tapering the dielectric as shown in Fig. 10. Even when both of the above measures were taken, we found it necessary to allow 0.7 mm/kV at 200 MHz when Teflon was used for the dielectric. The ultimate dielectric material is sapphire but it requires diamond tooling. Figure 11 shows how the feedthrough capacitors and a variable inductor are incorporated into the circuit of Fig. 6.

SUMMARY AND CONCLUSIONS

We have demonstrated that one can construct a broadband tunable double-tuned NMR probe utilizing lumped-element equivalents of transmission lines that is more efficient than a probe employing $\lambda/4$ transmission lines. With the lumped-elements approach one can vary the relative efficiency of the observe side vs the decoupling side of the probe by changing the ratio of the inductance of the sample coil to that

of the stop coil. The observe S/N is generally slightly better than that obtained with the $\lambda/4$ version, and the decoupling power is reduced by a factor of 3. Finally, because of the relatively high efficiency with respect to the utilization of ^{1}H-decoupling power, one would expect that the present design would be useful for "solids" at fields as high as 8.5 T.

ACKNOWLEDGMENTS

The authors gratefully thank the National Science Foundation Regional Nuclear Magnetic Resonance Facility at the University of South Carolina (CH78-18723) and the National Institutes of Health (GM26295) for partial support of this research. We also wish to acknowledge helpful comments from a referee concerning the section on S/N.

REFERENCES

1. V. Cross, R. Hester, and J. Waugh, *Rev. Sci. Instrum.* **47**, 1446 (1976).
2. M. Stoll, A. Vega, and R. Vaughan, *Rev. Sci. Instrum.* **48**, 800 (1977).
3. "CRC Handbook of Chemistry and Physics," 57th ed., CRC Press, Cleveland, Ohio, 1977.
4. D. Hoult and R. Richards, *J. Magn. Reson.* **24**, 71 (1976).
5. D. Traficante and J. Simms, *J. Magn. Reson.* **24**, 71 (1976).
6. C. P. Poole, "Electron Spin Resonance," Interscience, New York, 1976.
7. "The Radio Amateur's Handbook" (D. DeMau, Ed.), ARRL, Newington, Conn., 1979.
8. "Microwave Transmission Circuits' (G. L. Ragan, Ed.), Vol. IX, MIT–RLS, Boston, 1964.
9. H. Schneider and P. Dullenkopf, *Rev. Sci. Instrum.* **48**, 68 (1977).
10. J. J. O'Dwyer, "The Theory of Electrical Conduction and Breakdown in Solids Dielectrics," Oxford Univ. Press (Clarendon), London/New York, 1973.
11. J. C. Anderson, "Dielectrics," Spottiswoode, London, 1964.
12. W. J. Roff and J. R. Scott, "Fibres, Films, Plastic and Rubbers," Butterworths, London, 1971.

Reprinted from Journal of Magnetic Resonance **43**, 399–416 (1981)